Airgun-OBS Seismic Refraction Profiling Experiment(?)

Tôhoku Geophys. Journ. (Sci. Rep. Tôhoku Univ., Ser. 5), Vol. 28, Nos. 3-4, pp. 143-159, 1981

Airgun-OBS Seismic Refraction Profiling Experiment (I)

KIYOSHI SUYEHIRO*, HIDEKI INATANI**, TOSHIHIKO YAMADA***
and HIDEKI SHIMAMURA**

* Observation Center for Earthquake Prediction, Faculty of Science, Tohoku University, Sendai, 980, Japan
** Laboratory for Ocean Bottom Seismology, Faculty of Science, Hokkaido University, Sapporo, 060, Japan
*** Geophysical Institute, Faculty of Science, University of Tokyo, Tokyo, 113, Japan

(Received October 5, 1981)

Abstract: We have conducted a refraction profiling experiment using an airgun as a controlled source and an OBS (ocean bottom seismometer) as a receiver in the region off Sanriku coast of northern Japan in May, 1980. The main purpose of our experiment was to investigate the dependence of waveforms of airgun signals recorded by the OBS on various parameters such as airgun towing depth, air pressure, and air chamber size to gain in knowledge of an optimum setting of these parameters for clearer delineation of the seismic structure. It is found, as predicted from theory, that the predominant frequency and the signal duration are sensitive to airgun shot depth, which must be kept constant at an optimum depth to produce the same waveform with sufficient energy to penetrate the sea bottom.

A model of the upper crustal structure of the region is presented from a digital data analysis employing the simple delay-and-sum technique.

Introduction

To reveal seismicity and the velocity structure beneath an oceanic region is the main objective of marine seismological observations using ocean bottom seismometers (OBS's). When using the OBS data, we are often confronted with the problem of travel time correction for the local shallow seismic structure beneath an OBS site underlain almost inevitably by a low velocity sedimentary layer with a large Vp/Vs ratio. An airgun-OBS refraction survey reveals the velocity structure beneath the OBS and travel time corrections can easily be obtained. Once the locality is known, the data can be used to complement long range explosion data or to correct for natural earthquakes data.

As compared with much more powerful dynamite source, airgun shots are more accurately time controlled, have better waveform reproducibility, less dangerous, and require less expensive cost. In light of these advantages, the airgun source will not be limited for use as described above, but is a likely candidate to become a major tool to reveal deeper structure possibly to the uppermost mantle (Takeda, 1978; Shibuya and Miyashita, in prep.). From the receiver side, an OBS is advantageous over a surface hydrophone as the OBS is located in a more quiet environment (Avedik and Renard, 1973; Ibrahim and Latham, 1978) and can also record converted shear wave

arrivals to obtain S wave velocities as well, which are extremely important in constraining the possible range of crustal material.

An operation of airgun – OBS system has started at the Observation Center for Earthquake Prediction, Tohoku University in 1980 in cooperation with the Laboratory for Ocean Bottom Seismology, Hokkaido University, and Geophysical Institute, University of Tokyo. The first experiment was conducted off Sanriku coast in May, 1980. It was aimed to study the airgun wave form dependence on various parameters which could be controlled "on board" to search for an optimum source signal to be detected by OBS, and to obtain the crustal structure beneath the region.

Data Acquisition System

The airgun – OBS seismic refraction profiling experiment was conducted in the area as shown in Fig. 1, which is on the continent side of the Japan Trench where the water depth range is about 150 to 1000 m. In the following the operation of the refraction survey system is described (Fig. 2).

i) OBS: The OBS used in this experiment is a free-fall, pop-up type with timed release mechanism employing electrolytic dissolution. A vertical velocity sensor with 4.5 Hz natural frequency is mounted on gimbals inside the glass sphere housing. A 4 ch. cassette tape recorder, into which high-, middle-, and low-gain signals from the amplifier and BCD time code (Inatani and Furuya, 1980) are fed, runs for about 10 days when a C–90 tape is used (Shimamura and Asada, 1975; Yamada, Shimamura, and

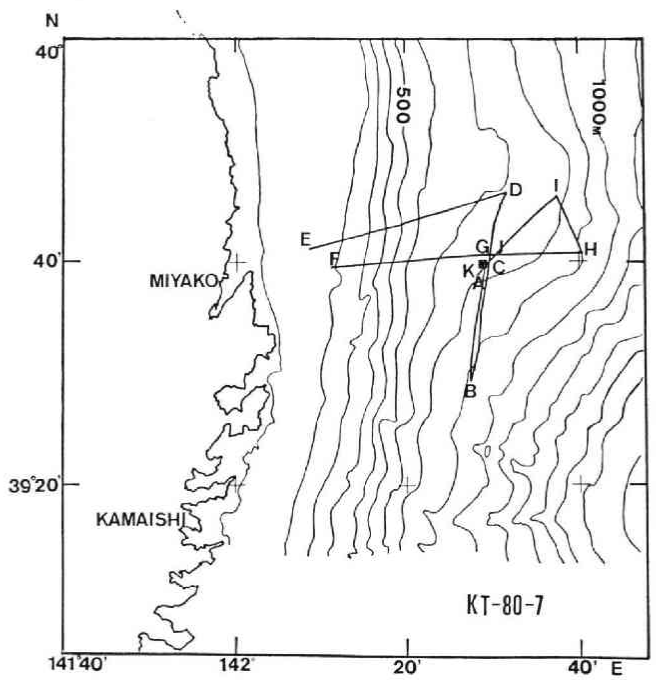

Fig. 1. Bathymetry map of the surveyed area. Solid square indicates the OBS location.

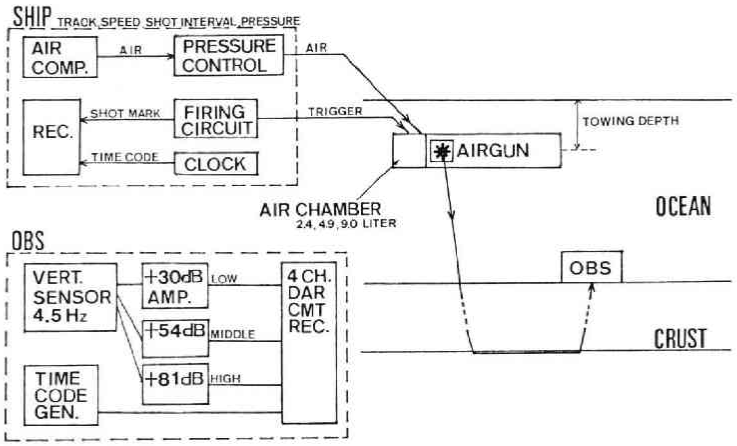

Fig. 2. Schematic view of the airgun – OBS refraction profiling operation. Pressure, air chamber volume, and towing depth characterize the shot waveform. Ship speed and shot time interval determine shot spacing.

Asada, 1976). A complete description of the system can be found in Yamada (1980). The OBS was deployed on the location shown in Fig. 3 on May 23 and retrieved on May 24, recording a total of about 400 airgun shots.

ii) AIRGUN: Highly compressed air of about 10 MPa pressure is supplied to the airgun via the air pressure controller located in the lab. Each airgun shot is fired by an electric trigger pulse which opens the solenoid valve and exhausts the compressed air stored in the pressure chamber into water. The generation of the trigger pulse is controlled by quartz clock and the shot time interval is kept constant.

In this experiment the compressor capacity was such that it required about 50 s to fire the airgun with 2.4 liter air chamber at 8–10 MPa. This shot time interval is much longer than would be contaminated by a previous shot, and therefore, the compressor was run at the maximum rate and shot spacings were determined by ship speed. The shot time intervals were set at 90 and 180 s for 4.9 and 9.0 liter air chambers, respectively at 8–10 MPa. The shot spacings were 100–150, 180–420, and 370–740 m for 2.4, 4.9, and 9.0 liter air chambers, respectively.

The airgun shot pulse was tape recorded together with JJY (standard time radio signal) calibrated clock pulse. The air pressure was checked from the pressure gauge for each shot.

While profiling we have altered air chambers and towing depth to test their effect on OBS records of airgun signals. The towing depth was controlled by ship speed. Normally the ship speed should be kept constant during a profile for minimum shot position error. Because of ship speed alterations, this experiment required a careful determination of the airgun – OBS distance as described below.

iii) SHIP TRACK: Fig. 3 shows the ship track. Water depth varied between 150

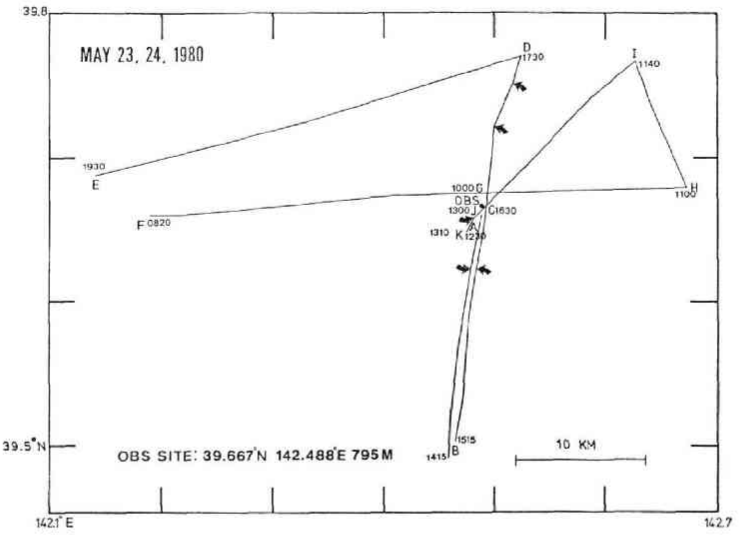

Fig. 3. Blow up of the ship track in Fig. 1. Times are indicated for points A through K. Arrows are indicated at positions where the ship speed was changed.

and 1000 m (Fig. 1). The ship was equipped with a LORAN C receiver and its readings and the direct water wave travel times were combined to obtain accurate positions. As the LORAN C system gives reliable position for the surveyed area, a position error would be at worst cases on the order of magnitude of 0.1 nautical mile.

Airgun Shot Signals

One of the merits using an airgun is its reproducibility of the signal which allows such data processing as velocity filtering. However, to generate desired airgun signals we must know their wave form dependence on such parameters as output pressure, air chamber volume, and shot depth.

The airgun is an explosion type which produces an air bubble which oscillates at a predominant frequency dependent on pressure, depth, and volume of the airgun. The predominant frequency can be expressed as,

$$f = c\, P_0^{5/6}(PV)^{-1/3}, \tag{1}$$

where c is a constant, P_0 is ambient pressure, P is chamber pressure, and V is chamber volume (Schulze-Gattermann, 1972). Ziolkowski (1970) predicts waveforms of airgun signals from a theory of a spherical bubble oscillation allowing for a finite amplitude oscillation. He predicts a longer signal duration with shot depth as one of the features and is experimentally proven (Ziolkowski, 1970; Mayne and Quay, 1971; Smith, 1975).

We have obtained OBS records of airgun waveforms for various settings of the above parameters (Table 1). The above equation indicates that the predominant frequency is more sensitive to arigun depth than to chamber pressure for a given volume

of airgun (Fig. 4). Fig. 5 shows examples of OBS records for similar OBS – airgnu distances and output pressures but different shot depths corresponding to different ship speeds. Differences in waveform are clearly observed from filtered traces; higher frequencies are more pronounced with lower ship speed. Note that the refraction arrival signal about 3 seconds before direct water phase for the shallowest shot depth (ship speed 17 km/h) is almost unobservable. Fig. 6 shows example records for different air chamber volumes to compare with Fig. 5, which indicate the features predicted from theory; increase in predominant frequency with larger shot depth and smaller chamber volume, and longer signal duration with depth. The amplitude decays with distance but the predominant frequency little changes for the distance range surveyed (Fig. 7). Fig. 8 shows the dependence of the predominant frequency of

Table 1.

Profile	Span	Chamber Volume	Mean Ship Speed
A – B	20 km	2.4 liter	8 km/h
			12
B – D	30	4.9	12
			17
			14
			9
D – E	34	4.9	17
F – H	42	9.0	15
H – I	11	9.0	15
I – K	19	9.0	15
			8

Airgun Firing Pressure: 7.8–10.8 MPa

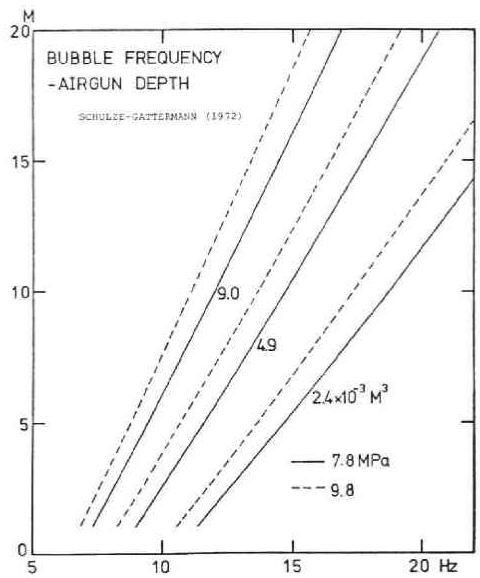

Fig. 4. Bubble frequency vs. airgun shot depth for three chamber volumes and characteristic pressures.

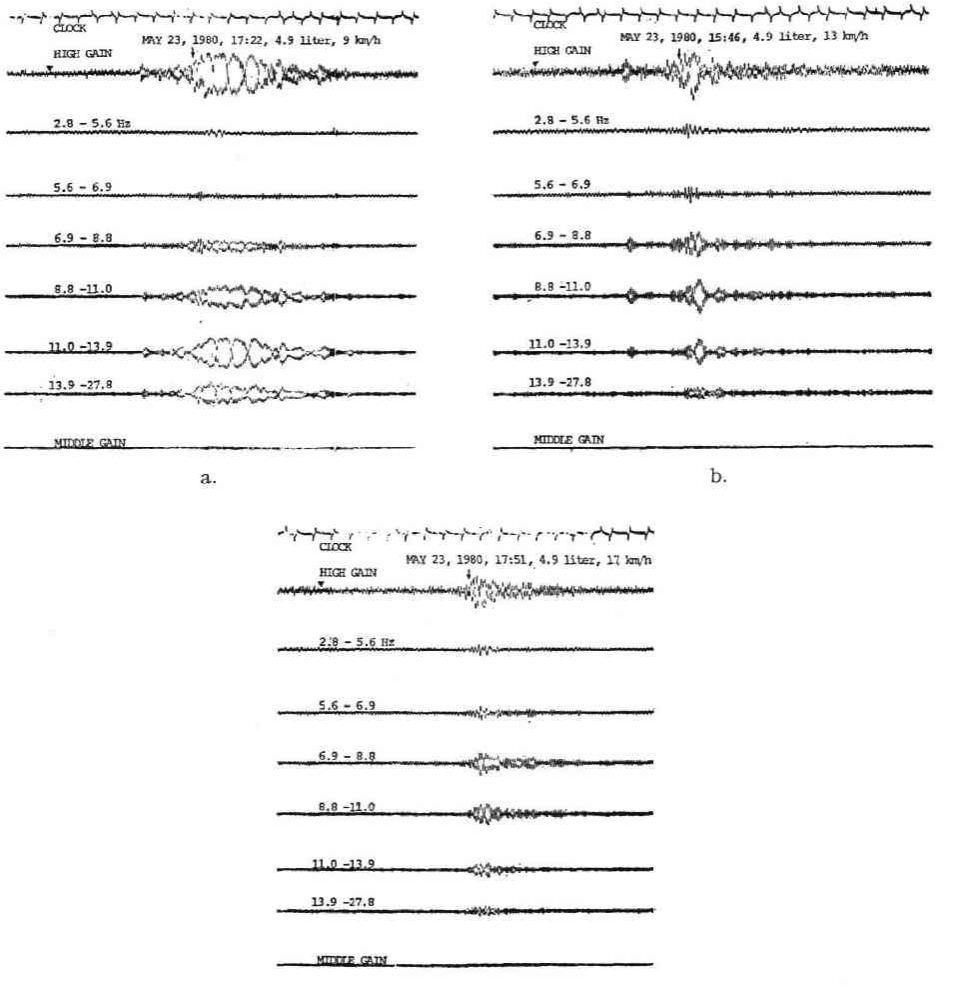

Fig. 5. Examples of OBS records for 4.9 liter air chamber shots at similar distances and pressures but different shot depths. Shot times and direct water wave arrivals are indicated by triangles and arrows, respectively. Higher predominant frequency and longer signal duration can be seen for lower ship speed, i.e. larger depth. At 17 km/h, not much energy penetration beneath ocean bottom is observed.

OBS records on ship speed. The predominant frequency was obtained using a spectrum analyzer applying a Hanning window (4 s.) and averaging 8 or 16 shots. The airgun shot depths, then, could be estimated from Fig. 4 and are plotted in Fig. 8.

Noise

Fig. 9 shows noise spectra of the survey area recorded by our OBS. The lowest level is at about 35 Hz and increases to both ends. The frequency response of the recorder system is flat between 2 to 30 Hz (3 dB points) (Yamada, 1980) and the overall OBS response curve is flat between about 7 to 30 Hz. Therefore, the spectra outside

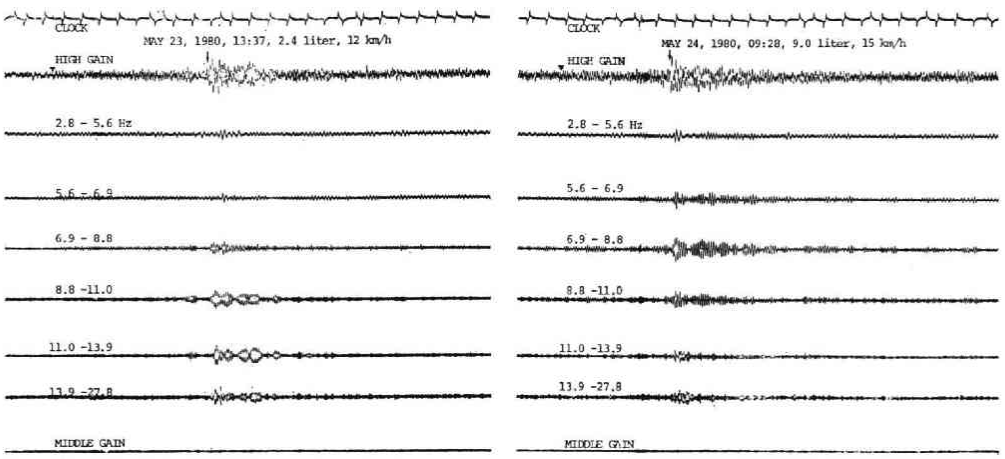

a. b.

Fig. 6. Examples of OBS records for 2.4 and 9.0 liter air chamber shots. Compared with Fig. 5, change in predominant frequency with chamber size can be seen.

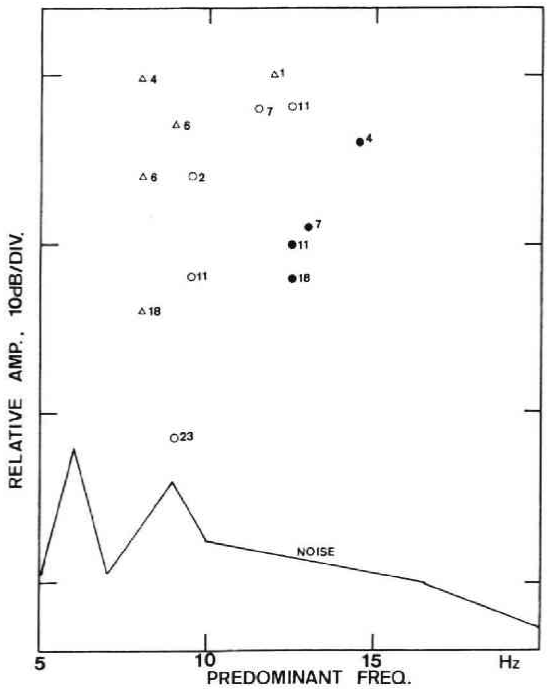

Fig. 7. Signal amplitude vs. predominant frequency. Solid circles, open circles, and triangles correspond to 2.4, 4.9, and 9.0 liter air chambers, respectively. Amplitude level decays with distance (figures attached to symbols), but predominant frequency little changes for this distance range.

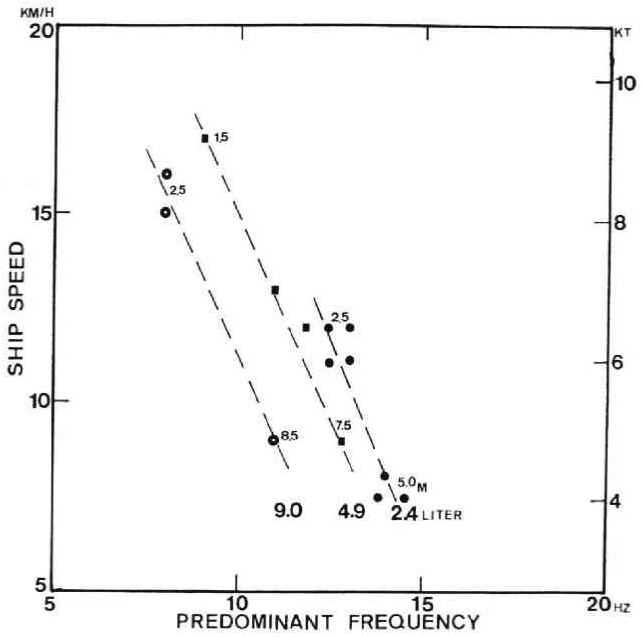

Fig. 8. Ship speed vs. predominant frequency. Towing depths estimated using Fig. 4 are also shown. For 2.4 liter shots, depths are shallower than for other chambers at the same ship speed because the towing wire length was shorter.

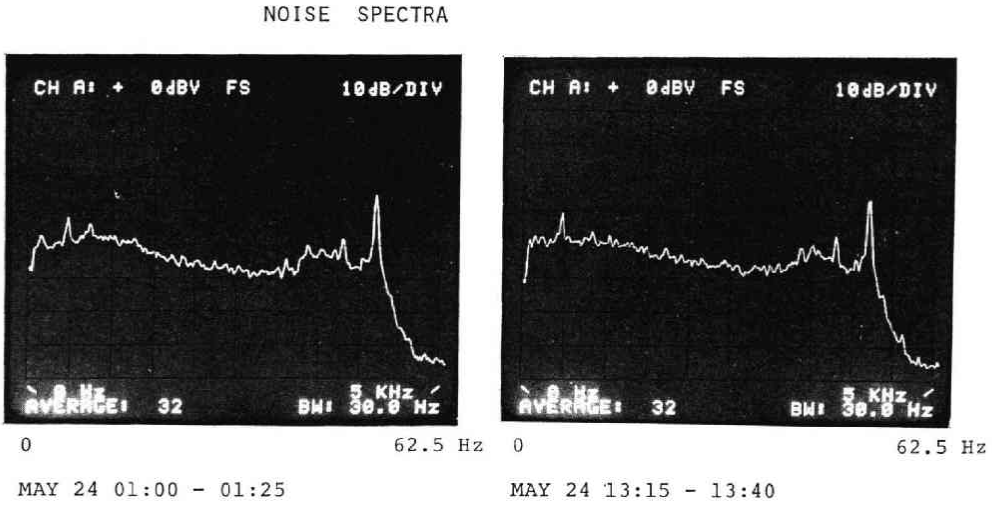

Fig. 9. Noise spectra of OBS record. Each division of horizontal axis corresponds to 6.25 Hz.

this range is not meaningful in this discussion. Within the above range, it can be said that the noise decreases monotonically with frequency. Noise spectra are important not only because they determine the threshold level but can vary regionally and temporally. For this region, a predominant frequency higher than 10 Hz would have

resulted in better S/N ratio since the signal is less than 10 dB above noise at 20 km distance including the water wave signal (Fig. 7).

Record Sections

i) DISTANCE: In this experiment, the ship speed was intentionally altered so that the distance between shot point and OBS is liable to a considerable error. Therefore, we used distances calculated using water wave arrivals readings together with those from coordinates determined from LORAN C readings. The acoustic speed in water can be determined by looking at distance dependence of the difference between the two distances. It is shown that a sound velocity in water of 1.46 km/s gives only a DC shift of less than 0.5 km between the two determinations, which were corrected for, and thus a reliable distance estimate could be achieved.

ii) DATA PROCESSING: Table 2 depicts the digital data processing procedure. Obviously a direct A/D conversion after cassette tape playback is desirable but it is beyond our present computer capability. Data stacking is a summation of five consecutive shots each delayed an amount of time interval appropriate for the stacking apparent velocity. This procedure enhances the signal with the stacking velocity and is a simplest type of velocity filtering.

iii) RECORD SECTIONS: Figs. 10–14 show the record sections of profiles AB, BC, CD, FG, and GH. The effect of shot depth is apparent from a change in overall darkness of these records due to a change in frequency content. A distinct change in waveform occurs at a distance of 4.5 km for profile AB where the predominant frequency moves to lower frequency (Fig. 10) (Table 1). Similar phenomena occur at 5 km for BC (Fig. 11) and at 10 km for CD (Fig. 12). The reverberation is more pronounced with depth as predicted by Ziolkowski (1970).

Fig. 10-a, b compares the same profile data with and without stacking. The stacked record section shows improvement of S/N ratio for arrivals with apparent velocity of 4.0 km/s. Such improvements are also observed in the data for other profiles (Figs. 11 and 13).

Despite the largest air chamber volume, refraction arrivals are less clear for profiles FG and GH compared to others. This is probably due to shallow shot depth and long shot spacing. Therefore, we use the records of profiles AB, BC, and CD to determine a model of the velocity structure of the region.

Table 2.
Data Processing Procedure

1:	DAR data cassette tape playback (approx. $\times 320$ real time)
2:	DAR open reel tape duplicate for speed reduction and original tape protection (playback at approx. $\times 80$ real time)
3:	Analog filtering (approx. 2.8–28 Hz real time)
4:	A/D conversion (approx. 16.1 ms real time sampling) (Nyquist freq. 31 Hz)
5:	Data stacking (five traces) (optional)
6:	Plot out ((gain at distance X)/(gain at distance 0)$=1+(0.07*X)^2$)

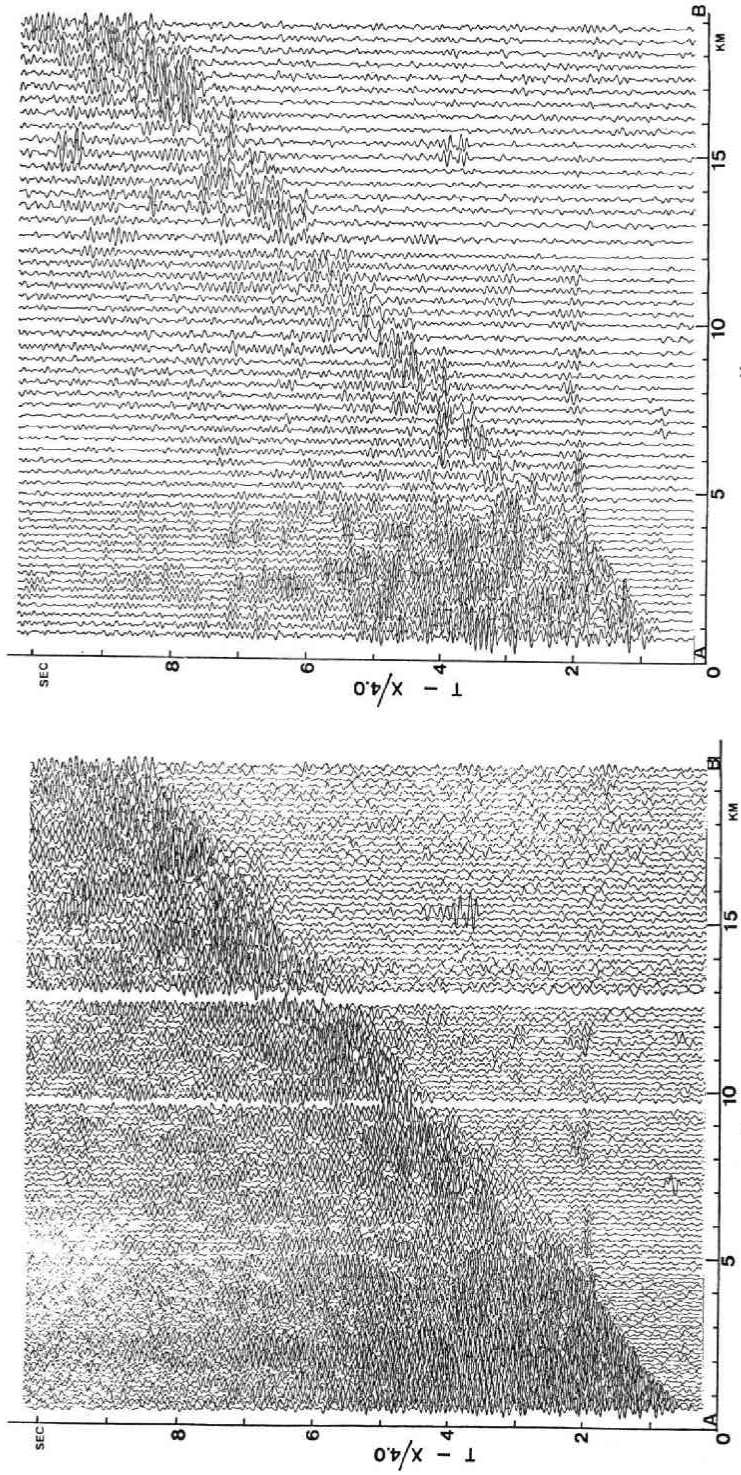

Fig. 10. OBS record sections for profile AB. a) records without stacking, b) records with five records stacked to enhance 4.0 km/s apparent velocity (not all are plotted).

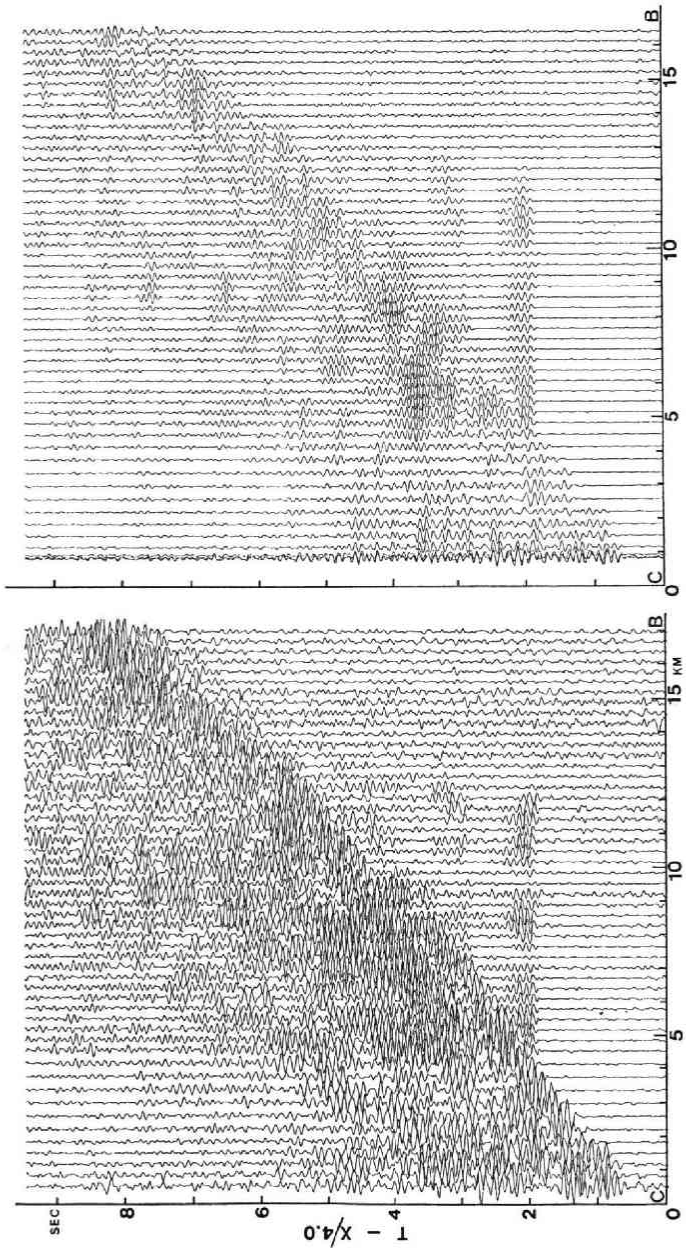

Fig. 11. OBS record sections for profile BC. See Fig. 10 for detail.

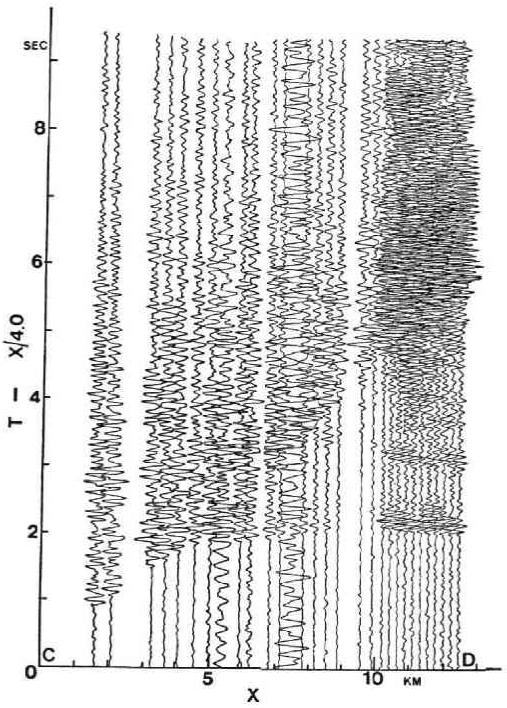

Fig. 12. OBS record section for profile CD.

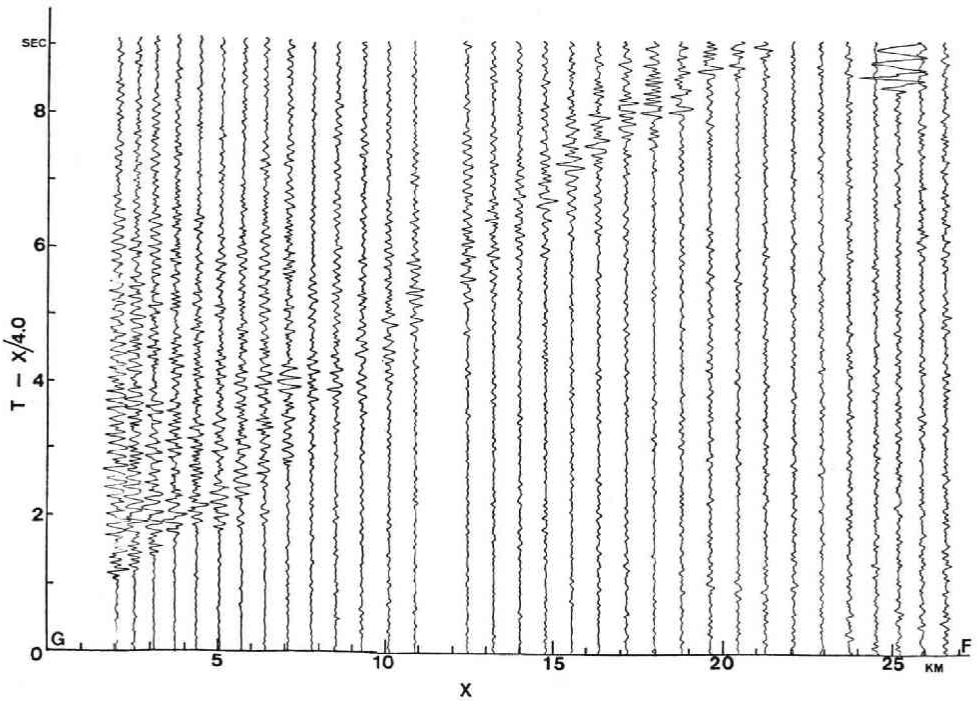

Fig. 13. OBS record section for profile FG.

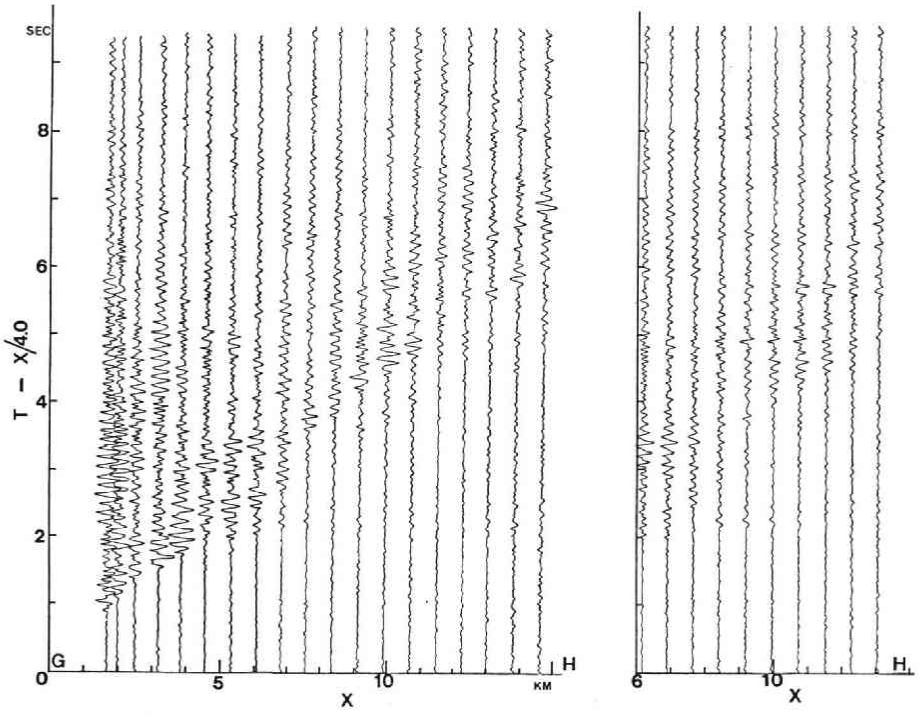

Fig. 14. OBS record sections for profile GH. See Fig. 10 for detail.

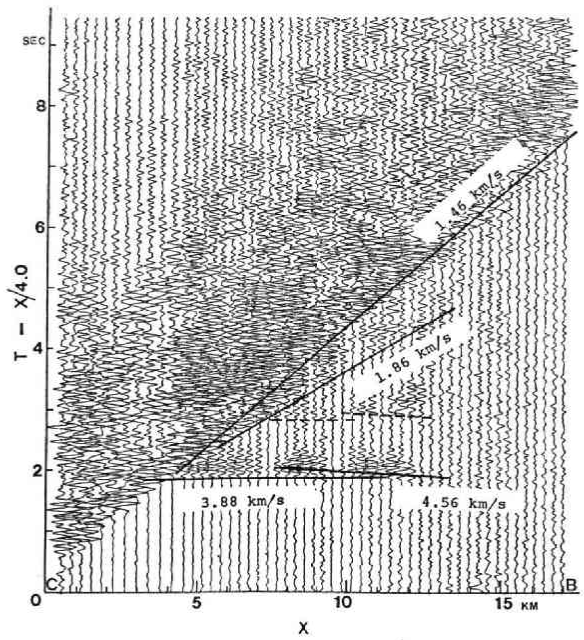

Fig. 15. Interpretation of the record sections for profile AB.

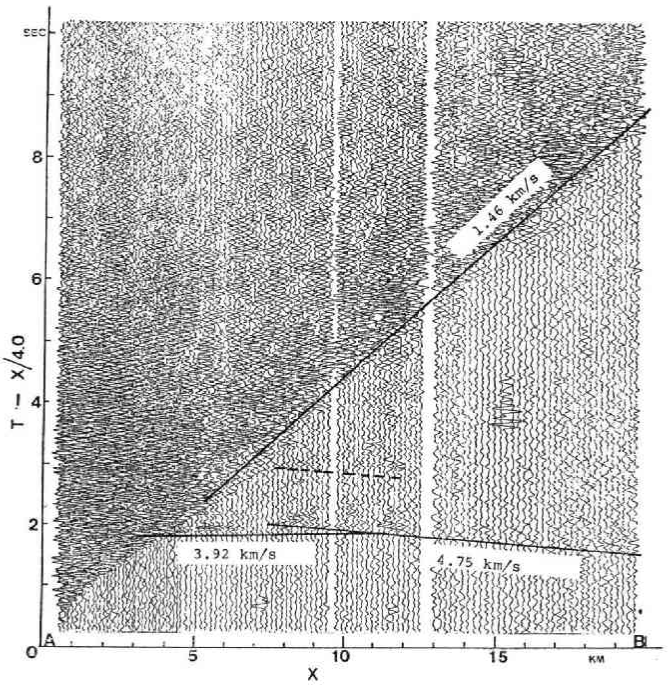

Fig. 16. Interpretation of the record sections for profile BC.

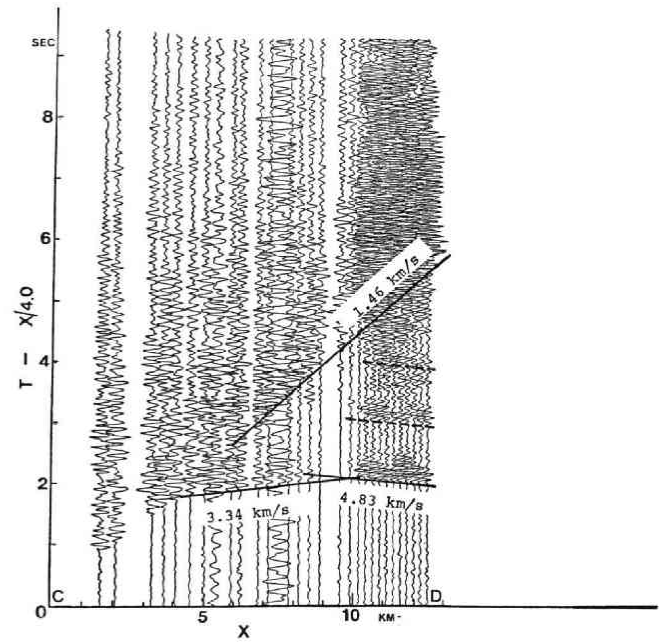

Fig. 17. Interpretation of the record section for profile CD.

iv) VELOCITY STRUCTURE: Because the main aim of our experiment was to obtain the dependence of OBS recorded signal waveform on various airgun parameters settings, we could not obtain the best results for velocity structure determination. Figs. 15–17 show our interpretation of the data.

All the profiles AB, BC, and CD show an apparent velocity larger than 4.5 km/s in the distance range of 10–12 km and the phase can be traced to 20 km distance in profile AB. The apparent velocity of the sedimentary layer is not well constrained. However, a choice of probable apparent velocity does not significantly change the depth of the highest velocity layer as the thicknesses of the above two layers are complementary. Profile CD indicates an apparent velocity of 3.3 km/s which may be indicative of a dipping interface since the corresponding velocities from profiles AB and BC are considerably higher. We, however, do not include it in our model as the profile CD is more complex than others because of drastic change in ship speed and a bend in the ship track. Table 3 depicts our preliminary model of the region.

Table 3.

1		2		3	
Velocity	Thickness	Velocity	Thickness	Velocity	Thickness
Water	0.79 km	Water	0.33 km	Water	1.33 km
1.90 km/s	1.4	1.55 km/s	0.74	1.95 km/s	1.78
		2.0	0.34		
		2.3	0.60		
3.9	1.5	3.6	0.93		
		4.2	1.39		
4.7		5.1	1.21	5.05	4.1
		5.8		5.90	

1: This paper
2: Profile SB–2 in Murauchi et al., 1980.
3: Profile P–6 in Ludwig et al., 1966.

Discussions

Shor (1963) states that the optimum firing depth for the maximum signal from explosions is to fire it at a depth equal to a quarter wavelength for the bubble pulse frequency. This is to avoid the erosion of the primary pulse by its surface reflection. This depth corresponds to about 16, 19, and 22 m with predominant frequencies of about 23, 20, and 17 Hz for 2.4, 4.9, and 9.0 liter airguns, respectively (Fig. 4). However, this should be considered the upper limit because an order of magnitude difference in amplitude can easily occur between, say, 10 and 20 Hz due to the effect of Q.

For a typical sedimentary layer velocity of 2 km/s, a 10 Hz signal has 0.2 km wavelength. As the layer thickness can be comparable to this wavelength a predominant frequency higher than 10 Hz would improve resolution. If the layer thickness is thinner, it will have only a negligible effect on seismic wave travel time. Taking these and the frequency response of the OBS into account, our experiment, although it did not cover sufficient shot depth range, seems to indicate that the shot depths greater than

about 3, 5, 10 m should be maintained for 2.4, 4.9, and 9.0 liter airguns, respectively.

Larger shot depth with a single airgun means less attenuation of bubble oscillation. A tuned array system of airguns with different predominant frequencies can suppress this unwanted pulsation. Also, in the course of data analysis, the knowledge of the source waveform would help eliminate the unwanted effect. These are the next steps to consider.

The shot depths were estimated after the experiment from Fig. 4 and observed predominant frequencies. They may be estimated "on board" from towing wire length or the time for the bubble to reach the sea surface. However, as the shot depth is the major controlling factor of the waveform, it seems essential to monitor gun depth by a pressure sensor. We have done such an experiment and the results wil be reported in a subsequent paper. Briefly, the shot depths may be slightly overestimated in this experiment.

Profiles AB and BC which run north to south are practically the same profile but with different chamber volumes, and therefore, constitute good examples to compare with. BC indicates better S/N ratio as expected but cannot identify 4.7 km/s phase at farther than 12 km distance. The phase can be traced on AB probably because the signal is pronounced farther than a distance of 27 km wheras BC does not extend as far, and because the shot spacing is shorter. Although the shot depths for the 9.0 liter airgun were too shallow to delineate a seismic structure, we can still observe arrivals of 4 km/s apparent velocity (Fig. 14) and it should be used to reveal the deepest structure with an optimum parameter setting. There was an operational restriction from the compressor capacity which required a three min. shot interval. Provided that the shot depth can be controlled by other means than the ship speed, larger compressor capacity is important as it reduces ship time and shot spacing, and can increase shot pressure.

The surveyed region lies on about the same latitude but further landward of the region extensively studied by Ludwig et al. (1966). Murauchi et al. (1980) have obtained a velocity structure model along latitude 38°35'N and their westernmost profile is in a similar water depth range. Their results are given in Table 3 for comparison. Our results are in general agreement with their results. More surveys in the region are necessary with more efficient airgun operation to reveal deeper velocity structure in light of the tectonic background of the region.

Acknowledgements: The authors thank Mr. T. Asanuma of Chiba University and Mr. C. Igarashi of Ocean Research Institute, University of Tokyo for their help in actual airgun operation. The authors thank Prof. S. Murauchi of Chiba University for his kind advice. The authors are grateful to Prof. T. Hirasawa for his encouragement throughout the experiment. The authors express their gratitude to captain, officers, and the crew of R/V Tansei of Ocean Research Institute, University of Tokyo for their help in the cruise KT-80-7. Finally, the authors thank Prof. A. Takagi for his warm support and Dr. A. Hasegawa for critically reviewing the manuscript.

References

Avedik, F. and V. Renard, 1973: Seismic refraction on continental shelves with detectors on sea floor. *Geophys. Prospecting*, **21**, 220–228.

Ibrahim, A.K. and G.V. Latham, 1978: A comparison between sonobuoy and ocean bottom seismograph data and crustal structure of the Texas shelf zone. *Geophys.*, **43**, 514–527.

Inatani, H. and I. Furuya, 1980: A microprocessor controlled time code generator for an OBS system. *J. Phys. Earth*, **28**, 281–292.

Ludwig, W.J., J.I. Ewing, M. Ewing, S. Murauchi, N. Den, S. Asano, H. Hotta, M. Hayakawa, T. Asanuma, K. Ichikawa, and I. Noguchi, 1966: Sediments and structure of the Japan Trench. *J. Geophys. Res.*, **71**, 2121–2137.

Mayne, W.H. and R.G. Quay, 1971: Seismic signatures of large air guns. *Geophys.*, **36**, 1162–1173.

Murauchi, S. and W.J. Ewing, 1980: Crustal structure of the Japan Trench: The effect of subduction of ocean crust. *Initial Reports of the Deep Sea Drilling Project, Vol. LVI, LVII.*, 463–469.

Schulze-Gattermann, R., 1972: Physical aspects of the "airpulser" as a seismic energy source. *Geophys. Prospecting*, **20**, 155–192.

Shibuya, K. and K. Miyashita, in prep.: Observation to Pn refracted waves from a large air gun with an ocean bottom seismometers in the Sea of Okhotsk.

Shimamura, H. and T. Asada, 1974: A cassette recorder for an ocean bottom seismometer. *Geophys. Bull. Hokkaido Univ.*, **32**, 17–24.

Shor, G.G., 1963: in *The Earth beneath the Sea, The Sea, Editor, M.N. Hill, Interscience Publishers, Vol.* 3, 20–38.

Smith, S.G., 1975: Research note, Measurement of airgun waveforms. *Geophys. J.R. astr. Soc.*, **42**, 273–280.

Takeda, K., 1978: Seismic exploration studies using air-guns and ocean-bottom-seismometers. -Development of the data-processing system and its application to surveys in the northwest Pacific Basin-. *M. Sci. dissertation to Hokkaido University*, pp. 62.

Yamada, T., H. Shimamura, and T. Asada, 1976: Resolving power of OBS recording system using compact cassette magnetic tape in determining time difference between signals in separate channels. *Zisin*, **29**, 287–297.

Yamada, T., 1980: *Ph. D. dissertation to University of Tokyo*, pp. 228.

Ziolkowski, A., 1970: A method for calculating the output pressure waveform from an air gun. *Geophys. J. R. astr. Soc.*, **21**, 137–161.